Magnetic properties of 3d pyrite-type mixed crystals calculated by the full-potential KKR-CPA method

2007 J. Phys.: Condens. Matter 19 365215

(http://iopscience.iop.org/0953-8984/19/36/365215)

IOP PUBLISHING JOURNAL OF PHYSICS: CONDENSED MATTER

J. Phys.: Condens. Matter **19** (2007) 365215 (6pp) doi:10.1088/0953-8984/19/36/365215

Magnetic properties of 3d pyrite-type mixed crystals calculated by the full-potential KKR-CPA method

M Ogura and H Akai

Department of Physics, Graduate School of Science, Osaka University, 1-1 Machikaneyama, Toyonaka, Osaka 560-0043, Japan

E-mail: ogura@phys.sci.osaka-u.ac.jp

Received 23 January 2007, in final form 21 March 2007
Published 24 August 2007
Online at stacks.iop.org/JPhysCM/19/365215

Abstract

The electronic and magnetic properties of pyrite-type mixed crystals $M_{1-x}M'_xS_2$ (M, M′ = Fe, Co, Ni) were investigated by use of the full-potential Korringa–Kohn–Rostoker (KKR) method combined with the coherent potential approximation (CPA). The results well explain the systematic behaviour of these systems as long as they are in a metallic phase. It is also concluded that the full-potential treatment is necessary to describe these anisotropic systems.

1. Introduction

Pyrite-type 3d transition metal compounds have drawn much attention for a long time due to their variety of electronic and magnetic properties. The electrical and magnetic properties of these systems are strongly affected by d-band filling. Thus FeS_2 is a semiconductor [1], but CoS_2 is a metallic ferromagnet [2, 3]. On the other hand, NiS_2 is considered as a Mott insulator of charge-transfer type [4, 5]. These behaviours are rather consistent with the electronic structure obtained by band structure calculations [6]: for FeS_2, the dϵ band is completely filled and the Fermi level is located in the band gap opening up between the dϵ and dγ bands. The dγ band is quarter filled for CoS_2, which ensures that the system becomes metallic. The situation is rather different for the NiS_2 case, where the dγ band is half filled. Since the on-site Coulomb interaction of Ni is considerably larger than the dγ band width, the system becomes a Mott insulator [6].

Another systematic change in the electrical and magnetic behaviours is observed by replacing the chalcogen from S to Se and Te for a fixed transition metal element. In this case, the systematic change is caused by a broadening of the dγ band: the band width increases on going from S to Se and further to Te. Accordingly, $CoSe_2$ is a metallic paramagnet with Curie–Weiss-type susceptibility [7], whereas CoS_2 is a ferromagnetic metal; $NiSe_2$ is a Pauli paramagnet [8–10], whereas NiS_2 is an antiferromagnetic (or weak ferromagnetic) semiconductor.

0953-8984/07/365215+06$30.00

Even more interesting cases are the mixtures of these systems, such as $Fe_{1-x}Co_xS_2$, $Co_{1-x}Ni_xS_2$ and $Co(S_{1-x}Se_x)_2$. For example, $Fe_{1-x}Co_xS_2$ shows a nonmagnetic-to-ferromagnetic transition in the low-concentration region of Fe [2, 3]. $Co_{1-x}Ni_xS_2$ shows metamagnetic behaviour in the vicinity of $x = 0.1$, where it loses the ferromagnetism [3]. $Co(S_{1-x}Se_x)_2$ also shows metamagnetism in the low-concentration region of Se before it undergoes a ferromagnetic-to-paramagnetic transition with increasing Se concentration [7].

In the present study, we investigate the magnetic behaviours of these alloy systems on the basis of the full-potential Korringa–Kohn–Rostoker (KKR) first-principles electronic structure calculation [11, 12] combined with the local density approximation (LDA) and the coherent potential approximation (CPA) [13, 14]. In the past, calculations based on LDA were performed for pure systems such as FeS_2, CoS_2 and $CoSe_2$ [6, 15], but not for alloy systems. Since a variety of magnetic and electrical behaviours is obtained through their constituent and concentration, a calculation for mixed crystals is indispensable for reaching a basic understanding of the pyrite-type transition metal compounds.

2. Calculation

Calculations were performed in the framework of the full-potential KKR Green's function method [12] combined with CPA. MX_2 pyrite-type crystal structure is rather loosely packed and is difficult to treat in a spherical potential model such as the muffin-tin potential approximation (MTA) and atomic–sphere approximation (ASA). Actually, the spherical potential model gives a total energy that monotonically increases or decreases, never showing minima, as the crystal lattice constant increases. Yamada *et al* realized a large packing fraction by introducing empty atoms and obtained a reasonable lattice constant within ASA [15]. However, they needed as many as 24 empty atoms in a unit cell, which consists of four M and eight X atoms. In their calculation of CoS_2, the critical lattice constant for the instability of the magnetic moment is rather large compared to the experimental one: their calculation shows that CoS_2 is paramagnetic with their optimized lattice constant, while it is ferromagnetic experimentally. Thus, we cannot determine both lattice and magnetic structures simultaneously with spherical models.

In the present study, we performed the full-potential calculation in order to overcome this problem. The lattice constants are determined without introducing any empty atoms for each combination and concentration of elements from the condition that the total energy is minimum. The lattice constants thus obtained are summarized in figure 1. The theoretical values are consistent with the experimental values [16], though the former are a little smaller than the latter due to LDA. The full-potential calculation also reproduces experimental magnetic structures well with the lattice constants obtained, as will be described in the next section. Here, the positional parameter u is fixed to be 0.389, because the experimentally observed variation in u is not large.

The effects of a mixed crystal were described within CPA [13, 14]. The systems dealt with are not fully disordered: only four of the 12 sublattices are occupied randomly by component atoms. In the present study, the KKR method combined with CPA was generalized for such cases.

In addition to the density of states and magnetic moments, the magnetic transition temperature (Curie temperature T_C) was estimated in the framework of the mean-field approximation: $T_C = 2/3\Delta E$, where ΔE is the total energy difference between the ferromagnetic and paramagnetic states. In the present systems, we used the total energy for the nonmagnetic state instead of the paramagnetic state, because the local moment disorder states were not obtained in these systems.

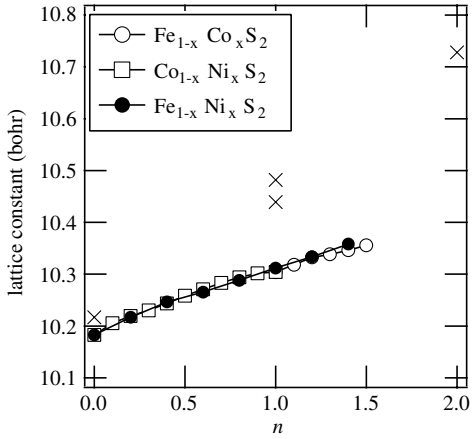

Figure 1. Calculated crystal lattice constants versus the averaged number of electrons n. The crosses mean the experimental value [16, 17].

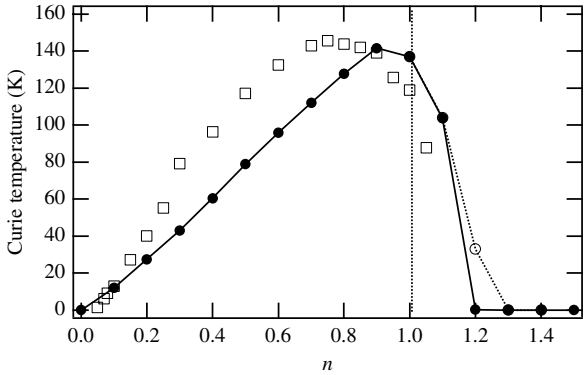

Figure 2. Curie temperature versus the averaged number of electrons n. The squares are the experimental values [2] and the circles are the theoretical values, respectively. The open circles are the results for the metamagnetic state.

3. Results and discussions

The calculated Curie temperatures are shown in figure 2 as a function of the averaged number of electrons in the dγ band n: $n = 0$, $n = 1$ and $n = 2$ mean FeS_2, CoS_2 and NiS_2, respectively. The behaviour of the theoretical Curie temperature reproduces that of the experimental results fairly well [2]: FeS_2 ($n = 0$) is nonmagnetic, but a finite value of T_C is obtained for $x \geqslant 0.1$. Then it increases as n increases. T_C has its maximum value slightly before n reaches unity and then decreases. Finally, the moment vanishes at $n \sim 1.1$.

The total and partial magnetic moments are summarized in figure 3. For $Fe_{1-x}Co_xS_2$, the behaviour of the calculated magnetic moment also reproduces that of the experimental magnetic moment. The magnetic moment is proportional to the Co concentration x over the range $0.1 \leqslant n \leqslant 0.9$, indicating that the magnetic moment is saturated (strong ferromagnetism) in this range. The magnetic moment at $x = 1$ is almost the same as that at $x = 0.9$. This means that the magnetic moment is no longer saturated for $x > 0.9$. The theoretical magnetic moments are slightly smaller than the experimental ones as a whole. This comes mainly from the fact that the theoretical lattice constants are smaller than the experimental lattice constants.

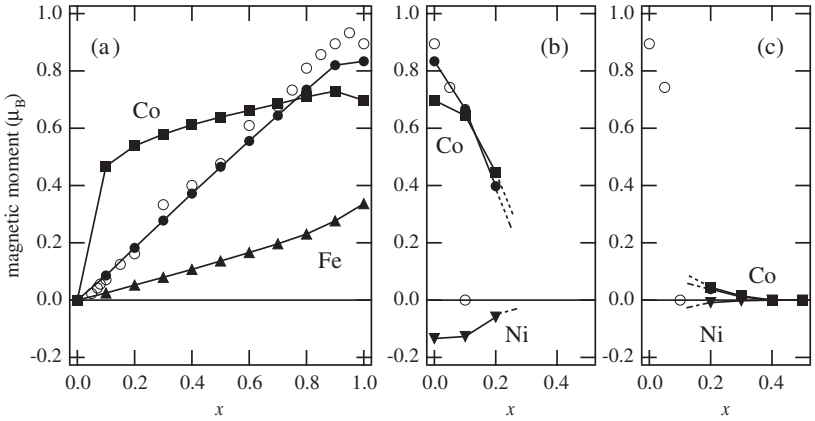

Figure 3. Magnetic moments of $Fe_{1-x}Co_xS_2$ (a), $Co_{1-x}Ni_xS_2$ (high spin) (b) and $Co_{1-x}Ni_xS_2$ (low spin). The open and closed circles are the experimental [2] and theoretical moments of the system, respectively. Other symbols indicate the theoretical moments at each atomic site.

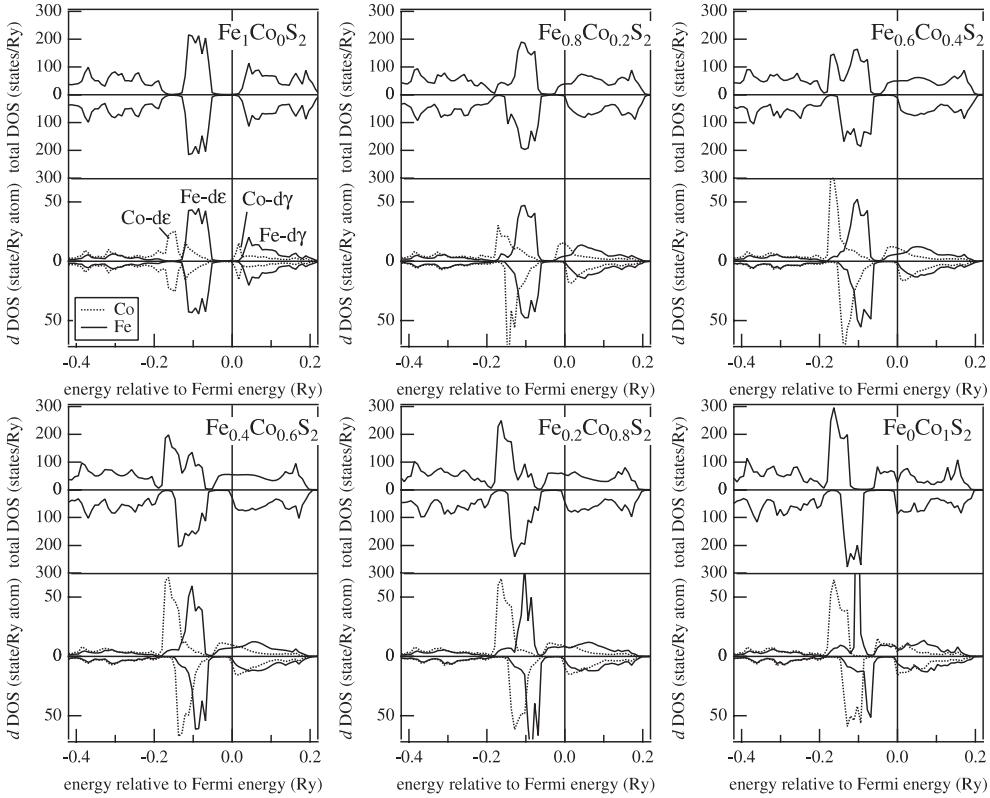

Figure 4. Total and partial 3d densities of states of $Fe_{1-x}Co_xS_2$.

As for the local magnetic moment within each atomic cell, Co atoms maintain a high value over the whole region of Co concentration, while the Fe moment increases along with the magnetization of the system.

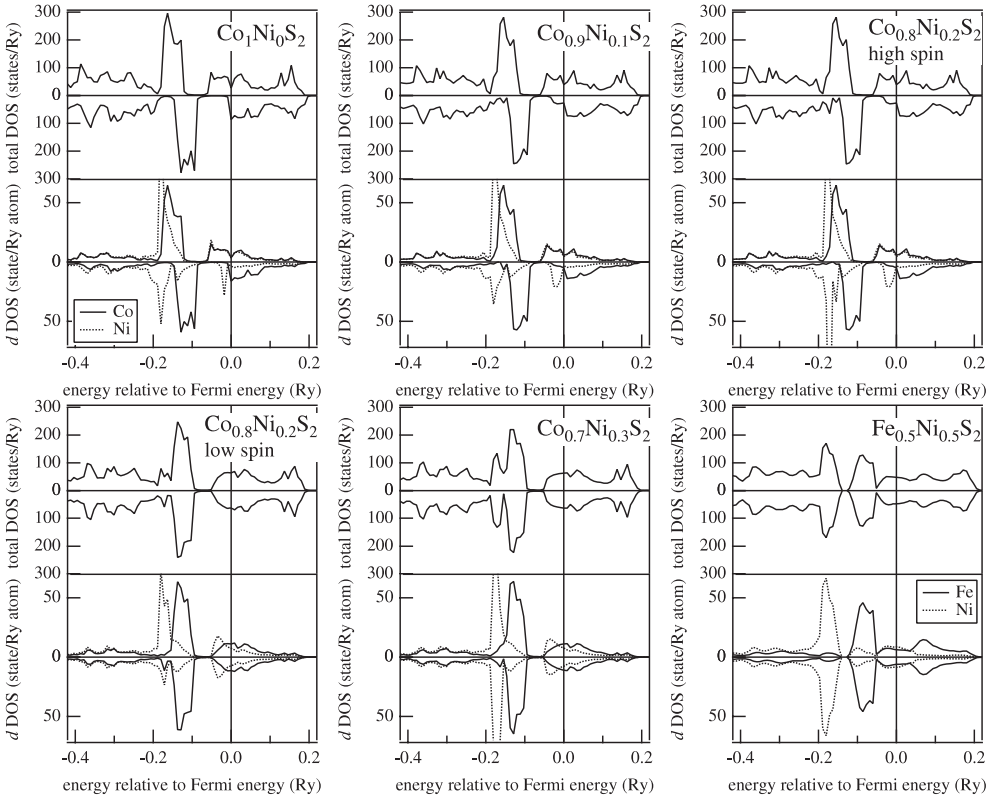

Figure 5. Total and partial 3d densities of states of $Co_{1-x}Ni_xS_2$ and $Fe_{0.5}Ni_{0.5}S_2$.

For $Co_{1-x}Ni_xS_2$, the magnetic moment decreases rapidly and disappears at $x \sim 0.2$ where T_C approaches zero. For $x \sim 0.2$, we obtained two kinds of stable magnetic states: high and low spin states. In Figure 2, the Curie temperatures for the high and low spin states are plotted by the open and closed circles, respectively. The existence of two magnetic states corresponds to the metamagnetic behaviour observed at the low Ni concentration region [7]. From figure 3, it is found that the magnetic moments of Co and Ni atoms couple antiparallel to each other for both the high and low spin states. We have not examined the antiferromagnetic or weak ferromagnetic state of NiS_2, since the Mott insulating behaviour of this system is outside the scope of the present framework of LDA.

The change in the magnetization reflects the change in the electronic state. Figure 4 shows the density of states (DOS) of $Fe_{1-x}Co_xS_2$. The upper half of each figure shows the DOS of the spin-up state and the lower half shows that of the spin-down state. As the Co concentration increases, the empty spin-up state is gradually occupied, whereas the number of electrons of the spin-down state does not change much. The polarization at the Fermi level is high and the situation is quite close to that of half-metals. At $x \sim 0.8$, the Fermi level reaches the shoulder of the down dγ state, which prevents the magnetic moment increasing further with increasing x. The densities of dγ states of Fe and Co are broad due to the hybridization between dγ states of Fe and Co atoms and hence the spin-up states of not only Co but also Fe are pulled down below the Fermi level due to the large Co spin polarization.

The DOS for $Co_{1-x}Ni_xS_2$ is shown in figure 5. The situation is quite different from that of $Fe_{1-x}Co_xS_2$. It is also clear from the DOS that the magnetic moments of Co and

Ni couple antiparallel to each other. In the ferromagnetic region (CoS_2, $Co_{0.9}Ni_{0.1}S_2$ and $Co_{0.8}Ni_{0.2}S_2$ (high spin) in figure 5), the DOS seems almost unchanged and the change in the total polarization of the system comes only from the change in the ratio of Co and Ni, whose magnetic moments couple antiparallel to each other. The magnetic moment of each site then suddenly disappears as the Ni concentration increases.

Another interesting system is $Fe_{0.5}Ni_{0.5}S_2$, which is isoelectric with CoS_2. Though CoS_2 is a metallic ferromagnet, $Fe_{0.5}Ni_{0.5}S_2$ behaves experimentally as a paramagnetic (Curie–Weiss-type) semiconductor [17]. The calculation, however, fails to reproduce this latter behaviour: the calculation shows that $Fe_{0.5}Ni_{0.5}S_2$ is a nonmagnetic (Pauli paramagnetic) metal. In figure 5, the DOS of $Fe_{0.5}Ni_{0.5}S_2$ is also shown. Here, the dγ band broadens due to disorder and neither a gap nor a 1/2-filling-subband structure is observed. It is not plausible that the metal–insulator transition takes place at this composition. We think that this might be due to a possible structural transformation or related to experimental uncertainties.

In conclusion, the full-potential KKR-CPA calculation explains the various electrical and magnetic behaviours of 3d pyrite-type mixed crystals well, as long as the systems are in a metallic phase. The full-potential treatment is indispensable for correct description of the anisotropic structure of these systems. On the other hand, there still remain some discrepancies between the theory and experiment in the insulating or semiconducting phases of the present systems (we put the trivial cases of the Mott insulator aside.) This point should be investigated further, both theoretically and experimentally.

Acknowledgment

This work is partly supported by Ministry of Education, Culture, Sports, Science and Technology KAKENHI, no. 17064008.

References

[1] Kou W W and Seehra M S 1978 *Phys. Rev.* **18** 7062
[2] Jarrett H S, Cloud W H, Bouchard R J, Butler S R, Frederick C G and Gillson J L 1968 *Phys. Rev. Lett.* **21** 617
[3] Ogawa S, Waki S and Teranishi T 1974 *Int. J. Magn.* **5** 349
[4] Kautz R L, Dresselhaus M S, Adler D and Linz A 1972 *Phys. Rev.* B **6** 2078
[5] Sato K 1984 *J. Phys. Soc. Japan* **53** 1617
[6] Bullett D W 1982 *J. Phys. C: Solid State Phys.* **15** 6163
[7] Adachi K 1991 *Physics and Engineering Applications of Magnetism* (*Solid State Science* vol 92) ed Y Ishikawa and N Niura (Berlin: Springer) p 83
[8] Bouchard R J, Gillin J L and Jarrett H S 1973 *Mater. Res. Bull.* **8** 489
[9] Kumada M, Mori N and Mitsui T 1977 *J. Phys. C: Solid State Phys.* **10** L643
[10] Czjzek G, Fink J, Schmidt H, Krill G, Lapierre M F, Panissod P, Gautier F and Robert C 1976 *J. Magn. Magn. Mater.* **3** 58
[11] Drittler B, Weinert M, Zeller R and Dederichs P H 1991 *Solid State Commun.* **79** 31
[12] Ogura M and Akai H 2005 *J. Phys.: Condens. Matter* **17** 5741
[13] Akai H 1989 *J. Phys.: Condens. Matter* **1** 8045
[14] Akai H and Dederichs P H 1993 *Phys. Rev.* B **47** 8739
[15] Yamada H, Terao K and Aoki M 1998 *J. Magn. Magn. Mater.* **177–181** 607
[16] Wyckoff R W G 1963 *Crystal Structures* 2nd edn (New York: Interscience)
[17] Adachi K, Ueno T and Tohda M 1976 *J. Phys. Soc. Japan* **41** 1069